Title
Emerging techniques and technologies in brain tumor imaging.

Journal
Neuro-oncology, 16 Suppl 7(Suppl 7)

ISSN
1522-8517

Authors
Ellingson, Benjamin M
Bendszus, Martin
Sorensen, A Gregory
et al.

Publication Date
2014-10-01

DOI
10.1093/neuonc/nou221

Peer reviewed

Neuro-Oncology

Neuro-Oncology 16:vii12–vii23, 2014
doi:10.1093/neuonc/nou221

Emerging techniques and technologies in brain tumor imaging

Benjamin M. Ellingson, Martin Bendszus, A. Gregory Sorensen, and Whitney B. Pope

Department of Radiological Sciences, David Geffen School of Medicine at University of California, Los Angeles, California (B.M.E., W.B.P.); Department of Biomedical Physics, David Geffen School of Medicine at University of California, Los Angeles, California (B.M.E.); Department of Bioengineering, Henry Samueli School of Engineering and Applied Science at University of California, Los Angeles, California (B.M.E.); Brain Research Institute, David Geffen School of Medicine at University of California, Los Angeles, California (B.M.E.); UCLA Neuro-Oncology Program, David Geffen School of Medicine at University of California, Los Angeles, California (B.M.E.); Department of Neuroradiology, University of Heidelberg, Heidelberg, Germany (M.B.); Siemens Healthcare, Erlangen, Germany (A.G.S.)

Corresponding Author: Benjamin M. Ellingson, PhD, Assistant Professor of Radiology, Biomedical Physics, and Bioengineering, Department of Radiological Sciences, David Geffen School of Medicine, University of California Los Angeles, 924 Westwood Blvd., Suite 615, Los Angeles, CA 90024 (bellingson@mednet.ucla.edu).

The purpose of this report is to describe the state of imaging techniques and technologies for detecting response of brain tumors to treatment in the setting of multicenter clinical trials. Within currently used technologies, implementation of standardized image acquisition and the use of volumetric estimates and subtraction maps are likely to help to improve tumor visualization, delineation, and quantification. Upon further development, refinement, and standardization, imaging technologies such as diffusion and perfusion MRI and amino acid PET may contribute to the detection of tumor response to treatment, particularly in specific treatment settings. Over the next few years, new technologies such as 2^3Na MRI and CEST imaging technologies will be explored for their use in expanding the ability to quantitatively image tumor response to therapies in a clinical trial setting.

Keywords: brain tumors, diffusion MRI, imaging biomarker, MRI, PET, perfusion MRI, response assessment, T1 subtraction.

Currently Available Techniques With Immediate Application

Standardization of Image Acquisition Reduces Variability in Measurements

In multicenter studies, the heterogeneity of MR scanners and parameters (eg, field strength, gradient system, manufacturer, sequences) must be considered. It is well known that even minor differences in hardware or in sequence timing may result in significant changes in image contrast and tumor measurements, potentially exceeding the changes caused by therapy or the disease itself. Furthermore, a variety of MR sequences are used for tumor assessment, which further hampers comparability between different centers without tight control and standardization of pulse sequence parameters.

A high contrast-to-noise ratio between tumor and surrounding tissue is crucial for precise measurement of tumor size. In addition to differences in sequences and sequence parameters,[1] lesion contrast is also dependent on the magnetic field strength of the scanner,[2] with higher field strengths showing higher contrast-to-noise compared with lower field strength scanners (eg, 3T vs 1.5T). Contrast-enhanced T1-weighted images show even higher variability, as the signal changes induced by the contrast agent are related to the timing, dose, and type of contrast agent used. Dynamic contrast-enhanced imaging has shown that the maximum contrast agent uptake occurs between 4 and 8 minutes after contrast agent application,[3] indicating that this is the most effective window for acquiring postcontrast T1-weighted images for minimal variability in lesion size estimation due to timing of contrast agent administration.

Volumetric Measurements of Enhancing Tumor Burden and Volumetric Enhancing Tumor Response to Therapy

There is increasing evidence to support the hypothesis that volumetric estimates of tumor burden are more accurate than 1D/2D measurements. A study by Voss et al[4] showed that the Macdonald assessment of chemotherapy resulted in a kappa coefficient of 0.51, with 55% of evaluated MRI studies not having a complete consensus for categorical tumor response measurement.[4] In a study by Shah et al[5], the best response assessment had a 63% correspondence between 1D and enhancing volume measurements and 69% correspondence between 2D and enhancing volume measurements. In a study comparing 1D, 2D (bidirectional),

Received 20 May 2014; accepted 18 July 2014

and 3D volumetric contrast-enhancing tumor measurements, only 3D enhancing volume was predictive of overall survival (OS) (along with age and sex).[6] Provenzale et al[7] showed poor reader agreement in tumor assessment, with an ~14% false-positive rate in the diagnosis of progression of tumors that are stable. A study comparing 1D, 2D, and 3D volumetric contrast-enhancing tumor measurements in childhood brain tumors showed relatively poor concordance between 3D and 1D/2D measurements of 61%–66%.[8] Others have reported somewhat higher concordance rates. For example, Galanis et al[9] compared 1D, 2D, and volumetric results and found good agreement between volume and linear measurements in terms of measurement response at 4 months for newly diagnosed gliomas (75% in 1D and 2D vs volumetric). Similar performance was observed when examining tumors treated with bevacizumab and concurrent irinotecan.[10] In general, high interobserver variability has been noted in bidirectional and unidirectional measurements compared with 3D measurements.[11] This is most likely due to difficulty defining the exact margins and identifying the largest diameter or perpendicular diameter[12] and the tendency of 1D/2D measurements to overestimate tumor volume,[6] thus leading to a significantly longer measured progression-free survival (PFS)[8] that is presumably due to larger estimates of tumor burden at baseline.

Volumetric Analysis of Recurrent Glioblastoma Treated With Bevacizumab

Results from volumetric analyses in recurrent glioblastoma (GBM) treated with bevacizumab appear to be mixed. A single-institution study by Ellingson et al[13] demonstrated that >75% of patients experienced a >5% decrease in contrast-enhancing volume after bevacizumab and that there was no link between the change in contrast-enhancing tumor volume and PFS or OS. In support of these findings, a recent ACRIN-6677/RTOG-0625 multicenter study presented by Boxerman et al[14] convincingly demonstrated that an increase in contrast-enhancing volume beyond 8 or 16 weeks can be used to predict OS in recurrent GBM treated with bevacizumab; however, a decrease in the volume of contrast enhancement (ie, "response") was not predictive of OS. These results are similar to a recent multicenter study by Ellingson et al[15] involving conventional volumetric segmentation of data from the BRAIN trial, showing that the change in enhancing volume before and after treatment with bevacizumab was not predictive of PFS or OS. In contrast to these studies, a single-institution study by Huang et al[16] recently found that baseline enhancing volume, posttreatment residual enhancing volume, and percentage change in enhancing volume were all predictive of PFS and OS. Together, these studies suggest that there are, at most, only weak correlations between volumetric response to bevacizumab and patient survival using conventional volumetric segmentation techniques.

3D Image Acquisition Further Reduces Variability in Lesion Volume Assessment Compared with 2D Acquisition

To date, most tumor studies are performed using 2D techniques with higher in-plane resolution than through-plane resolution (ie, slice thickness). It has been shown that incorrect repositioning of these slices increases variability of lesion volume estimates at follow-up,[17] and that this variability can be reduced by implementing automatic slice positioning tools. Alternatively, the use of 3D acquisition instead of 2D MRI sequences is thought to reduce variability relating to slice positioning by as much as 50%.[18]

Evidence suggests that the use of 3D T1-weighted MR images to evaluate tumor volume may have a significant impact on the evaluation of therapeutic benefit. For example, a recent study by Boxerman et al[14] demonstrated that early progression on both 2D and 3D T1-weighted images acquired 8 or 16 weeks following drug treatment using bevacizumab with irinotecan or temozolomide in recurrent glioblastoma (RTOG-0625) predicted OS; however, 3D T1-weighted images allowed for a better separation of responders and non-responders on Kaplan-Meier curves, presumably due to more accurate assessment of lesion volumes using 3D acquisition techniques.

Although 3D gradient echo-based sequences are by far the most commonly used in brain tumor clinical trials (eg, MPRAGE or SPGR sequences), 3D spin echo-based sequences (eg,f CUBE or SPACE sequences) may also be beneficial for quantifying lesion volumes. 3D spin echo-based sequences may have added benefits of reduced susceptibility artifacts and increased contrast-to-noise when used on contrast-enhanced T1-weighted imaging compared with 3D gradient echo-based sequences; however, 3D spin echo sequences typically suffer from lower signal-to-noise, higher specific absorption rate, and specific sequence acquisition details may vary across vendors due to lack of sequence standardization.

Contrast-enhanced T1 Subtraction (CE-ΔT1w) Maps Improves Visualization and Quantification of Enhancing Tumor

The use of image subtraction was first described by des Plantes in 1961[19] and continues to be useful for applications requiring detection of subtle changes in contrast uptake. In fact, the use of digital subtraction maps has been recommended by the American College of Radiology (ACR) and Society for Skeletal Radiology (SSR) in their guidelines for interpretation of MRI of bone and soft tissue tumors.[20] In the brain, digital subtraction of postcontrast MR images from precontrast MR images was described by Suto et al[21] as early as 1989. In 1993, Lloyd et al[22] demonstrated the utility of contrast-enhanced T1-weighted subtraction maps in head and neck tumors, showing that subtraction maps provide a more accurate record of tumor extent compared with unsubtracted postcontrast MR images. In a pictorial essay in 1996, Lee et al[23] described the use of image subtraction as a broadly applicable postprocessing technique that can be performed at any field strength and any T1-weighted sequence in a variety of imaging applications, including use in differentiating enhancing lesions from hemorrhage. Later that year, Gaul et al[24] examined subtraction maps in the presence of hyperintense subacute hemorrhage in the area of interest on T1-weighted images, noting a net negative signal within areas of blood products and net positive signal in areas of residual tumor on subtraction maps. A study by Melhem et al[25] in 1999 attempted to quantify the benefit of postcontrast T1-weighted subtraction maps compared with standard postcontrast images, noting that enhancing brain lesions

were more conspicuous on the subtraction images, had a significantly higher contrast-to-noise ratio, and could identify residual enhancement in 88% of patients with parenchymal hematomas where standard postcontrast T1-weighted images had failed.

A recent study by Ellingson et al[15] implemented a variation of this subtraction technique in order to estimate contrast-enhancing lesion volumes before and after bevacizumab therapy in recurrent GBM as part of the BRAIN trial. Results suggested that there were significant differences between conventional and T1-subtraction defined volumes, particularly when examining the change in contrast between pre- and posttreatment time points. Results showed that tumors exhibiting a decrease in contrast-enhancing volume had a significantly longer PFS and OS. The ability to predict PFS and OS was further improved when accounting for differences in the treatment paradigm (bevacizumab alone or in combination with CPT-11) and with the addition of a subsequent confirmatory scan. Together, these results suggest that T1 subtraction maps may be extremely useful for improving tumor delineation, visualization, and quantification of enhancing tumor even following changes in vascular permeability.

To date there are a variety of commercially available and open-source solutions for performing T1 subtraction. Since T1 subtraction is identical to digital subtraction angiography (DSA), many postprocessing workstations from MR system manufacturers are already equipped with digital subtraction capabilities. Additionally, third-party software packages are also available for T1 subtraction, including the open-source version of Osirix™.

Reproducibility, Reliability, and Accuracy of Contrast Enhancement, Volumetric Analysis, and T1 Subtraction Maps

Reproducibility of brain tumor volume measurements appears to be on the same order of magnitude as reported in the Alzheimer's Disease Neuroimaging Initiative (ADNI), an NIH/NINDS-sponsored initiative involving analysis of high-resolution 3D T1-weighted images of the human brain and the quantification of subtle changes in anatomical volumes and measurements. For example, a study by Kaus et al[26] performed both manual and automated segmentation of low-grade gliomas and noted intraobserver and interobserver coefficient of variations of ~2% and 13.6%, respectively, using manual segmentation; both were reduced to <3% after using an automated algorithm. This is similar to other automated techniques that have shown estimated tumor volume errors ranging from 2.5% to 10% compared with manual segmentation.[27] Quantification of 3D volumes from 2D-acquisition protocols appears to result in slightly higher variability in tumor volume measurements. A study by Mazzara et al[28] noted intraobserver variability of ~20% and interobserver variability of 28%, and a similar study by Weltens et al[29] showed a coefficient of variance ranging from 14% to 33% for tumor volumes on MRI, depending on whether the lesion volumes were determined by radiologists, radiation oncologists, or neurosurgeons. This range is similar to those determined on CT,[30] and on average results differed by ~1.5 cc.[31]

Preliminary comparison between volumetric segmentation of standard postcontrast T1-weighted images and T1 subtraction maps suggests that T1 subtraction provides a lower coefficient of variance compared with standard postcontrast T1 weighted images, regardless of whether a vascular permeability agent is used (Figure 2). In particular, a pilot study was conducted of 20 patients randomly selected from 2 different multicenter clinical trials involving antiangiogenic agents. Enhancing tumor volumes were segmented by 3 technologists with 2+ years of segmentation experience before and after administration of therapy. Results suggest that T1 subtraction maps reduce the coefficient of variance in both trials and both contexts compared with standard segmentation, and T1 subtraction maps provide a more dramatic reduction in variability when used for evaluation of tumor burden during antiangiogenic therapy. These results support the hypothesis that T1 subtraction maps improve the ability to delineate tumor burden regardless of therapy.

Although not specifically addressed in the literature, it is conceivable that use of 3D spin echo-based sequences may provide higher contrast-to-noise T1 subtraction maps when compared with subtraction maps generated from 3D gradient echo-based acquisition based on preliminary 2D comparisons. Despite this potential advantage, however, the use of 3D spin echo sequences are not currently common for volumetric contrast-enhanced T1-weighted imaging in glioblastoma. Future efforts focused on standardization of 3D spin echo sequences across vendors and direct comparisons with 3D gradient echo sequences are critical for integrating these potentially advantageous sequences into multicenter clinical trials.

Emerging Techniques That Require More Validation

Diffusion MRI

Diffusion-sensitive MRI techniques are another imaging method that has shown promise in predicting response to standard cytotoxic as well as modern antiangiogenic therapies. Diffusion-weighted imaging (DWI) is sensitive to microscopic, subvoxel water motion for which an apparent diffusion coefficient (ADC) can be estimated, reflecting the magnitude of water motion. ADC has been shown to be inversely correlated with tumor cell density,[32–34] largely thought to be due to restriction of extracellular water motion due to tightly packed tumor cells. Given that brain neoplasms have a higher cell density than normal tissues, they have lower ADC values. On the other hand, edema and necrosis, which are associated with lower cell densities, have relatively higher ADC values. This relationship, however, can be confounded by a variety of factors including ischemia,[35] differences in cell shape,[36] and the presence of infection or inflammation.[37]

Diffusion MRI Reflects the Degree of Malignancy

Although studies have shown an inverse correlation between tumor cell density and ADC, high-grade gliomas are spatially and genetically heterogeneous and show regions of high cellularity adjacent to areas of necrosis and edema. This degree of heterogeneity can hamper correct tumor grading through the use of diffusion MRI and has illustrated a limitation of using mean ADC as a measure of tumor malignancy.[38] Some studies have shown

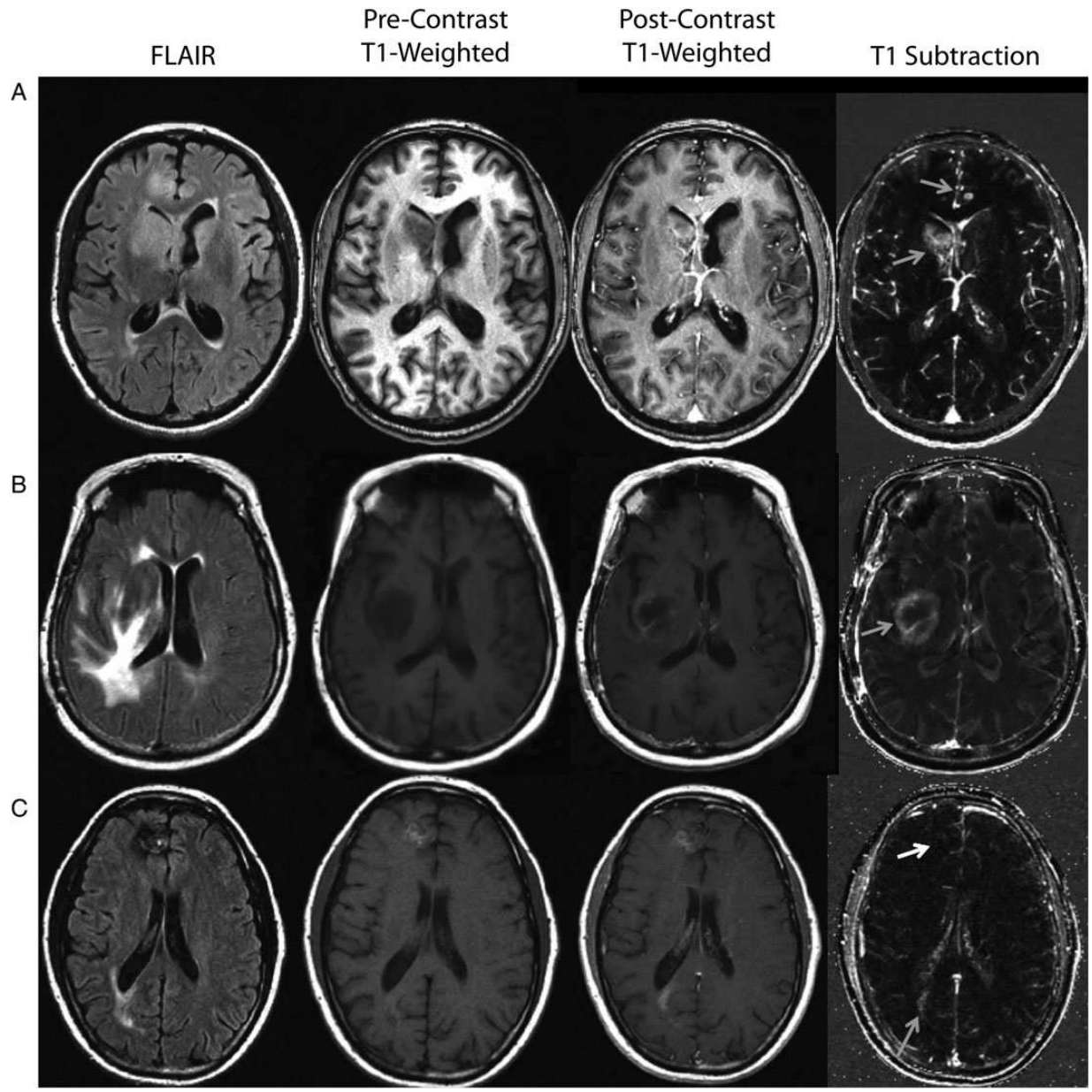

Fig. 1. Standard structural images and contrast enhanced T1-weighted subtraction maps in patients treated with bevacizumab at recurrence. (A) A patient with recurrent glioblastoma showing nonenhancing tumor near the right lateral ventricle after treatment with bevacizumab. This patient has multifocal disease including 2 potential diffuse cortical lesions identified on FLAIR. Postcontrast T1-weighted images show ill-defined regions of subtle contrast enhancement within these potential lesions. T1 subtraction maps clearly identify an enhancing mass near the right lateral ventricle, along with a single enhancing nodule within the cortex in the left frontal lobe (grey arrows). (B) A patient with recurrent glioblastoma showing extensive FLAIR signal changes and subtle contrast enhancement near the internal capsule after administration of bevacizumab. After application of T1 subtraction maps, the conspicuity of this lesion is clearly improved, and it can be identified as an obvious ring-enhancing lesion (grey arrow). (C) A patient with recurrent glioblastoma treated with bevacizumab showing 2 areas of concern, one in the right frontal lobe and the other in the right posterior lateral ventricle. With postcontrast T1-weighted images, both of these suspicious lesions show enhancement; however, precontrast T1-weighted images show T1 shortening consistent with blood products within the frontal lobe lesion. After application of T1 subtraction maps, the lesion in the frontal lobe is hypointense (white arrow), and the lesion near the posterior lateral ventricle is hyperintense (grey arrow). This example illustrates the ability of T1 subtraction maps to both identify subtle enhancing lesions as well as exclude blood product-related T1 shortening.

lower ADC in high-grade gliomas compared with lower grade gliomas;[33] however, other studies have reported considerable overlap between mean ADC values.[39] Thus it appears that diffusion MRI has sufficient sensitivity, but inadequate specificity, to accurately predict the degree of malignancy using mean ADC values.

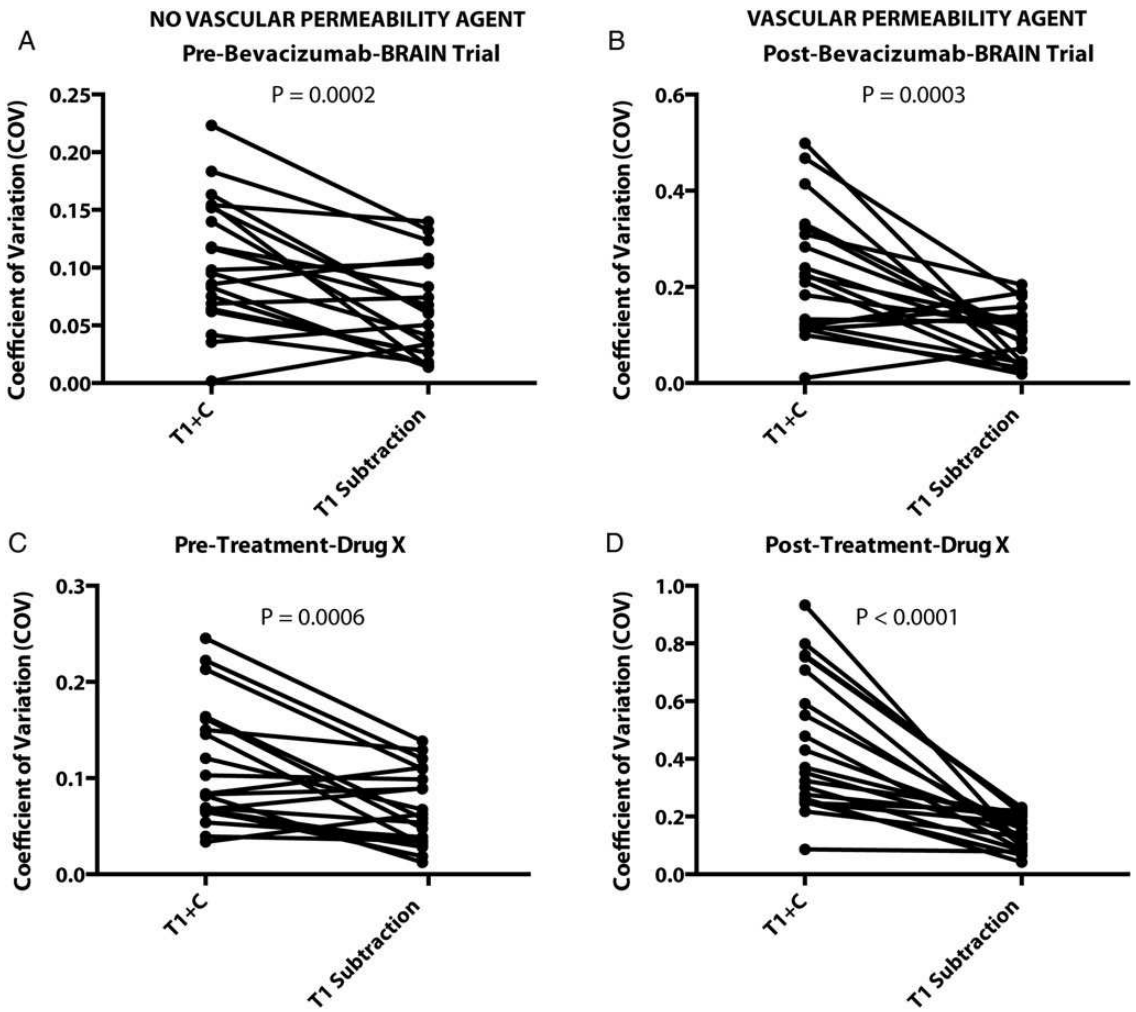

Fig. 2. Contrast-enhanced T1-weighted digital subtraction maps improve coefficient of variation (CV) in tumor volume quantification in both the presence of antiangiogenic agents as well as nonneoplastic agents. (A) CV in lesion volumes prior to administration of bevacizumab in the BRAIN trial showing a significant decrease in CV after calculation of subtraction maps (*t* test, *P*¼ .0002). (B) CV in lesion volumes after administration of bevacizumab in the BRAIN trial showing a significant decrease in CV in subtraction maps (*t* test, *P*¼ .0003). (C) CV in lesion volumes prior to administration of an undisclosed antiangiogenic agent showing significant decreases in CV in subtraction maps compared with standard postcontrast T1-weighted images (T1 + C) (*t* test, *P*¼ .0006). (D) CV in lesion volumes after to administration of an undisclosed antiangiogenic agent, showing significant decreases in CV in subtraction maps (*t* test, *P* < .0001).

Diffusion MRI as an Early Biomarker for Response to Cytotoxic Therapy and as a Tool for Differentiating Pseudoprogression From Tumor Recurrence

Early changes in ADC have been shown to be predictive of response to cytotoxic therapies, including radiation and antineoplastic therapies. Specifically, studies have shown that a transient decrease in ADC occurs after surgical resection due to ischemia and/or reactive cell hypertrophy,[40] and an increase in ADC following cytotoxic therapies has been shown to be associated with a favorable response[41] likely relating to destruction of cell membranes resulting in a decrease in restricted diffusion. Together, these studies suggest that diffusion MRI may add value in identifying tumors that are responsive to cytotoxic therapy and may provide added specificity for differentiating pseudoprogression from recurrent tumor.

Diffusion MRI in Antiangiogenic Therapy

Pope et al[42] utilized the distribution of ADC values within pretreatment contrast-enhancing regions to predict the response to bevacizumab. Specifically, this study fit a double Gaussian, mixture model to the ADC histogram extracted from pretreatment contrast-enhancing regions and noted that the mean of the lower ADC histogram, ADC_L, was a significant predictor of PFS. In a follow-up multicenter study, Pope et al[43] verified these findings and noted that lower mean ADC_L values were associated with shortened survival.

General Variability in ADC

Diffusion MRI estimates of ADC have been proposed as a possible surrogate for tumor cellularity, as changes in ADC have been

shown to be early predictors of various therapies. Using a temperature-controlled water phantom, Chenevert et al[44] noted a variance of ~5% in ADC measurements when examining various vendors, platforms, and field-strengths. This represents the minimum variability in diffusion measurements that can be obtained by the MR system. In ACRIN-6677/RTOG-0625, diffusion MRI was collected, and unpublished results from this study have suggested that normal CSF and NAWM mean ADC measurements have a coefficient of variance of ~7.3% and 10.5%, respectively. In the BRAIN trial, Pope et al[43] showed a coefficient of variance in lesion ADC of ~17%, and unpublished results demonstrated a wide variation in ADC measurements in NAWM across the various sites.

In summary, diffusion MRI is still considered an emerging technology because there remains a considerable lack of data regarding the effects of standardization of image acquisition parameters on diffusion measurements, lack of data regarding reproducibility in multicenter trials, and lack of data regarding how diffusion MRI measurements might best be integrated as a possible imaging endpoint.

Perfusion MRI

Perfusion MRI techniques have been used for nearly 20 years in the evaluation of malignant brain tumors and largely consist of 3 primary approaches: dynamic susceptibility contrast (DSC)-MRI, dynamic contrast enhanced (DCE)-MRI, and arterial spin labeling (ASL). DSC-MRI is a first-pass bolus imaging technique based on the indicator-dilution method and was introduced in the late 1980s[45] as a method of estimating relative cerebral blood volume (rCBV), flow (rCBF), and mean transit time (MTT) using the magnetic susceptibility properties of paramagnetic contrast agents (eg, gadolinium and other lanthanide chelates) and T2*-weighted MR acquisition methods. Various investigations have shown that these perfusion parameters reflect important biological information regarding tumor vascular morphometry.[46] Alternatively, DCE-MRI involves application of a pharmacokinetic model to describe the exchange of paramagnetic contrast agents between the vascular space and extravascular, extracellular space using the changes in longitudinal relaxation known to accompany paramagnetic contrast agents on dynamic T1-weighted images.[47] Although there are a few variations of this model, the primary variable of interest in most brain tumor studies is K^{trans}, the transfer coefficient between the intravascular space and the extravascular, extracellular space related to the product of vessel surface area and vascular permeability, but often used as a surrogate of vascular permeability in oncologic studies. A arterial spin labeling is a noninvasive method of estimating and quantifying (CBF)[48] that does not involve injection of contrast but instead uses magnetic tagging of blood water as an endogenous, diffusable tracer.

Perfusion MRI as an Early Biomarker for Radiotherapy Response

Perfusion imaging has also been investigated as a potential biomarker for early response to radiation therapy. Mangla et al[49] found that the percentage change in rCBV from the pre- and post-treatment measurements was predictive of 1-year survival with a sensitivity of 90% and a specificity of 60%. In a larger study, Law et al[50] found that rCBV could be used to predict time to progression. Cao et al[51] found that fractional tumor volume with high rCBV was predictive of survival in high-grade gliomas, in qhixh patients with a decrease in the fractional tumor volume with high rCBV from week 1 postradiation to week 3 postradiation had better survival outcomes than those who did not.

Perfusion MRI May Help in Predicting Pseudoprogression From Tumor Recurrence

The use of perfusion imaging to differentiate true progression from pseudoprogression has been an area of active investigation. Barajas et al[52] investigated DSC parameters as a means of differentiating recurrent glioblastoma from radiation necrosis (verified by histopathology) and noted that mean, maximum, and minimum rCBV were significantly greater in patients with recurrent tumor than in patients with radiation necrosis. Hu et al[53] examined the use of rCBV in differentiating glioma recurrence from radiation necrosis, showing a sensitivity of 91.7% and a specificity of 100% for differentiating these 2 conditions using a rCBV ratio threshold of 0.71. Sugahara et al[54] studied patients with new enhancing lesions that developed within irradiated regions to evaluate the effectiveness of rCBV in differentiating tumor recurrence from radiation necrosis, showing that normalized rCBV ratios >2.6 relative to white matter occurred in cases of recurrent tumor and ratios <0.6 in cases of radiation necrosis.

Perfusion MRI in Antiangiogenic Therapy

Several studies have focused on using perfusion imaging to assess response to antiangiogenic therapy; however, initial studies were disappointing in that there was no strong correlation between reduction in tumor perfusion and survival. For example, Sawlani et al[55] studied 16 patients with recurrent glioblastoma treated with bevacizumab and evaluated mean rCBV, mean leakage coefficient, and hyperperfusion volume (HPV), which is defined as the fraction of tumor with an rCBV above a prespecified threshold, as potential biomarkers for treatment response. They found that the percent change in HPV (using a rCBV threshold of 1.00) from baseline to first follow-up had a marginally significant hazard ratio of 1.077 when correlated with time to progression. Sorensen et al[56] studied 31 patients with recurrent glioblastoma treated with cediranib and explored a vascular normalization index by combining K^{trans}, microvessel volume, and circulating levels of collagen IV. Sorensen et al found that this new index (measured 1 day after treatment initiation) was closely associated with OS and PFS.

General Variability of DSC-MRI

DSC-MRI is commonly used in clinical assessment of malignant gliomas and cerebral ischemia and/or stroke; thus, much of the information regarding reproducibility and accuracy can be derived from the stroke literature. Despite preliminary data from relatively small studies, there remains a significant need to clearly validate DSC-MRI techniques and determine standardized methods that provide clinically reliable measurements across multiple institutions.[57] Generally speaking, reproducibility of DSC-MRI hemodynamic parameters across multiple institutions is difficult to achieve due to a wide range of issues that affect the sensitivity of the MR signal and derived parameters, including arterial

dispersion of the bolus occurring between the site of recorded arterial input function (AIF) and the position of the true AIF,[58] the concentration-dependent difference in T2* relaxivity between tissue and large vessels, and specific scan parameters including acquisition flip angle,[59] gradient-echo versus spin-echo preparation,[60] and echo time.[61]

When evaluated on the same scanner using the same acquisition protocol, DSC-MRI appears to be relatively consistent. A study by Henry et al[62] examined the test-retest reliability of DSC-MRI estimates of rCBV and noted a coefficient of variation of 14% in the cortex and 12% in subcortical regions. Shin et al[63] examined CBV and CBF measurements and noted a coefficient of variation of ~16% in normal white matter and 19% in gray matter. Additionally, a study by Jackson et al[64] examined the reproducibility of DSC-MRI estimates of rCBV and noted a 95% confidence interval of 12%–15% in test-retest evaluations. A mock multicenter study by Ellingson et al[65] examined the variation in DSC-MRI estimates of CBV when evaluated across various MR scanners, field strengths, and acquisition protocols during follow-up evaluations and noted a coefficient of variation of around 30% for raw CBV measurements, or ~25% when evaluated on the same scanner.

Effects of Contrast Agent Dose on DSC-MRI

The specific contrast agent dose used and the timing after injection can also cause variations in measured perfusion parameters. Alger et al[66] showed that a double dose of contrast resulted in approximately a 20% underestimation of rCBV and rCBF compared with a single dose. This appears to contradict a recent study by Paulson and Schmainda,[59] who noted that a single dose of contrast resulted in higher variability in rCBV when compared with double-dose administration.

Effects of Preload Contrast Agent Administration on DSC-MRI

In addition to contrast agent dose-related changes in perfusion parameters during MR acquisition, measurement can also be influenced by whether a preload or initial dose of contrast is used prior to dynamic acquisition. Knutsson et al[67] demonstrated that the use of a prebolus improves quantitative estimates of absolute CBF and CBV, even in healthy volunteers. Hu et al[68] showed a dramatic increase in accuracy of predicting radiation necrosis from recurrent tumor when using any size preload dose (>80% correctly diagnosed with preload vs 62% without the use of a preload). An animal study by Boxerman et al[69] also showed that the use of a preload reduced variability of intratumoral rCBV measurements approximately 8x when compared with iron oxide nanoparticles as a reference standard. Additional evidence suggests other factors related to preload dose delivery, including incubation time prior to dynamic acquisition, may influence the degree of T1-weighted leakage compensation and accuracy of rCBV measurement.[70]

Effects of Postprocessing on DSC-MRI

A variety of postprocessing techniques are available, and each can influence the measurement of tissue perfusion. Paulsen and Schmainda[59] noted that gamma-variate curve fitting tended to underestimate rCBV and trapezoidal integration without leakage compensation resulted in underestimation of rCBV. Studies have shown that singular value decomposition (SVD) methods for deconvolution tend to underestimate CBF when the AIF lags the concentration curve.[71] Thus, techniques including circular SVD[72] and Bayesian approaches[73] have been developed to further improve accuracy of DSC-MRI perfusion parameters. Furthermore, various institutions have demonstrated that different estimates of CBV/CBF often arise from identical regions of interest depending on the particular software package used (eg, IBNeuro, NordicICE, FuncTool) despite supposedly similar methods for leakage correction and curve fitting.

Normalization of DSC-MRI Parameters

Despite great effort in terms of absolute quantification of perfusion parameters using DSC-MRI, most of the parameters derived from DSC-MRI are relative measures. To overcome this limitation, some investigators have suggested normalizing these measurements to normal-appearing white matter or another reference tissue; however, other studies have demonstrated that this assumption may be prone to error due to variability of perfusion-normal white matter tissue.[74] Aware of this limitation, Bedekar et al[75] implemented a method of piecewise linear grayscale "standardization" of perfusion measures using a training dataset, noting a reduction in the variability from 9%–37% to 4%–6%. A study by Ellingson et al[65] compared various methods of postprocessing including the use of standardization and Gaussian normalization and noted a reduction in variability of CBV within malignant glioma tissue from 25% to 30% to less than 20%.

Interobserver and Intraobserver Variability of DSC-MRI

In one of the only studies examining interobserver and intraobserver variability in DSC-MRI, a study by Wetzel et al[76] examined the variability associated with measuring rCBV in 50 patients by 3 board-certified neuroradiologists These investigators noted an interobserver coefficient of variance of ~30% and an intraobserver coefficient of variance of 32%–41%, with variations between observers increasing with increasing rCBV values. Additionally, Wetzel et al note ~20% variation in rCBV measurements within normal-appearing white matter. In summary, there are many factors that influence the variability in DSC-MRI perfusion measurements in malignant gliomas.

General Variability of DCE-MRI in Brain Tumors

In July 2012, the Quantitative Imaging Biomarker Alliance (QIBA) created a white paper document outlining the use and quantification of DCE-MRI for clinical trials.[77,78](The specific recommendations of QIBA can be found at: http://www.rsna.org/uploadedFiles/RSNA/Content/Science_and_Education/QIBA/DCE-MRI_Quantification_Profile_v1%200-ReviewedDraft%208-8-12.pdf). The normal measurement variations, as well as recommended acquisition and postprocessing techniques, are well outlined in this document. Briefly, Ferl et al[79] explored the reproducibility of DCE-MRI perfusion parameters by obtaining a repeat baseline scan in recurrent glioblastoma patients prior to treatment with bevacizumab and noted a coefficient of variation of 13% for K^{trans} and 23.6% for v_e. A study by Roberts et al[80] documented a 13%–

19% coefficient of variation for K^{trans} and 11%–14% variation in v_e within human brain tumors, depending on the postprocessing technique and pharmacokinetic model used. Also, Jackson et al[81] investigated the reproducibility of DCE-MRI parameters and noted a coefficient of variance for K^{trans} of 7.7% and v_e of 6.2%.

Amino Acid Positron Emission Tomography

PET radiotracers have been used for the evaluation of brain tumors since 1982, when Di Chiro et al synthesized and used [^{18}F]-fluorodeoxyglucose (^{18}F-FDG) to characterize hypermetabolism in brain tumors.[82] An alternative target for molecular imaging of brain tumors involves labeling amino acids involved in protein metabolic pathways. Amino acid transport is increased in malignant cells;[83] which is hypothesized to be due the net result of increased demand for amino acids for amino acid synthesis for proliferation, transamination, and transmethylation, the use of amino acids as glutamine for fuel,[84] and as precursors for other biochemical syntheses. Regardless of the specific end use of these amino acids in brain tumors, various studies have shown that a wide variety of radiolabeled amino acids are useful for brain tumor molecular imaging. These tracers include [^{11}C-methyl]-methionine (^{11}C-MET), the most widely studied amino acid tracer in brain tumors to date,[85] L-1-[^{11}C]-tyrosine (^{11}C-TYR)[86], and other amino acids utilizing the longer half-life [^{18}F] radiolabel including O-(2-[^{18}F]-fluoroethyl)-L-tyrosine (^{18}F-FET)[87] and 3,4-dihydroxy-6-[^{18}F]-fluoro-L-phenylalanine (^{18}F-FDOPA)[88] (as well as the ^{18}F-FDOPA metabolite 3-O-methyl-6-[^{18}F]-fluoro-L-DOPA[89]). Although each of these amino acid uptake tracers are unique in the complexity of their synthesis as well as their precise involvement in protein synthesis and amino acid uptake pathways, numerous studies have demonstrated that they have very similar patterns of accumulation and performance in identifying regions of active tumor.[90] Studies have shown that amino acid PET may have the ability to differentiate tumor growth from treatment-related changes with a sensitivity of 75%–100% and specificity ranging from 60% to 100%.[91] Large multicenter studies are needed to verify these findings. Despite promising results, amino acid uptake can also be elevated in inflammatory processes, and it may be difficult to differentiate recurrent tumor from background tissue in many cases.[92]

Variability in Amino Acid PET Measurements

Relatively few studies have been performed using amino acid PET compared with previously mentioned imaging techniques, and no multicenter studies have been performed to date. In a well-summarized systematic review and meta-analysis of 13 studies consisting of 462 patients, Dunet et al[93] reported that high-grade gliomas had a tumor to normal brain 18F-FET PET coefficient of variance of ~38%. Chen et al[51] reported a coefficient of variance of tumor to brain uptake using 18F-FDOPA PET of ~29% in treatment-naïve high-grade glioma patients and 23% in post-treatment gliomas. Similarly, Singhal et al[94] reported a coefficient of variance of tumor to brain 11C-MET PET uptake of ~36% in high-grade gliomas. Together, these preliminary studies suggest amino acid PET has a relatively high variability within tumor tissues, even in single institution settings.

Techniques on the Horizon

^{23}Na MRI

Unregulated cell division of tumor tissue can be initiated by sodium/proton (Na^+/H^+) exchange kinetic changes and subsequently leads to alterations of Na^+/potassium (K^+) - ATPase activation. This results in elevated intracellular sodium concentration, which is correlated with tumor malignancy.[95] ^{23}Na MRI is able to reflect changes in tissue sodium concentration. Ouwerkerk et al[96] found an increased tissue sodium concentration (TSC) in brain tumors and perifocal edema compared with contralateral health tissue. Nagel et al[97] illustrated elevated TSC in WHO grade I–IV brain tumors, and showed that TSC strongly correlates with the tumor proliferation rate (MIB-1). However, clinical use of ^{23}Na MRI is currently not feasible due to the low resolution and the low SNR at clinical field strengths.

Chemical Exchange Saturation Transfer Imaging

Chemical exchange saturation transfer (CEST) imaging is a noninvasive MRI technique sensitive to endogenous mobile proteins and peptides, respectively, and their tissue specific concentration. Multiple metabolites (eg, glutamate, glutamine, creatine, myo-inositol, and other proteins) feature exchangeable protons and thus become endogenous agents with distinct chemical shifts, making CEST a technology with the potential for frequency-selective molecular imaging. Biomedical applications have already been demonstrated for the detection and grading of tumors.[98] Furthermore, CEST contrast has been reported to serve as a potential neuroimaging biomarker for proteins, peptides, amino acids, or pH.[99] Of these applications, CEST imaging appears to have great promise as a pH-weighted MRI technique[100] that is particularly attractive and would have immediate clinical benefit for monitoring treatment response, prediction of early treatment failure, identifying candidates for specific chemotherapies, and understanding the changes that occur in the tumor microenvironment during antiangiogenic therapies.

Conclusions

In summary, there are many currently available imaging technologies that may be implemented immediately to improve assessment of tumor response by increasing conspicuity the tumor and/or reducing the measurement variability. Additionally, there are a variety of promising physiological imaging technologies on the horizon, but these require further evaluation and standardization before being integrated into multicenter clinical trials for reliably evaluating new therapeutics.

Recommendations

† Pre- and postcontrast T1-weighted MR imaging sequences should be matched and standardized in future multicenter trials.
† Volumetric acquisition of T1-weighted images should be used for volumetric quantification of enhancing tumor burden.
† Contrast-enhanced T1-weighted subtraction maps should be a primary focus for further evaluation and validation as a

measure of enhancing tumor burden and assessment of response to therapy.

Additional Suggestions

- † The role of T2/FLAIR signal changes in assessing disease status should be reevaluated after T1 subtraction maps have been implemented, to determine if T2/FLAIR signal change continues to add value in evaluating response to therapy and if it outweighs the limitations of inherent subjectivity in assessing these changes.
- † Diffusion and perfusion imaging should be standardized in a multicenter trial setting for further investigation and validation as potential secondary imaging endpoints for response assessment.
- † Amino acid PET imaging should be investigated in a multicenter trial once limitations on its availability are overcome because of its potential to identify metabolically active enhancing and nonenhancing tumor.
- † More accurate measures of tumor burden should be developed to allow for identification of drugs and interventions that slow, rather than reverse, tumor growth.

Funding

Ellingson – Genentech/Roche Research Grant; Siemens Research Grant. Bendszus – None. Sorensen – None. Pope – Genentech/Roche Research Grant.

Conflict of interest statement. Ellingson – Genentech/Roche, Siemens Healthcare. Bendszus – None. Sorensen – Siemens Healthcare (employee). Pope - Genentech/Roche, Amgen, Guerbet, Celldex Therapeutics.

References

1. Wintersperger BJ, Runge VM, Biswas J, et al. Brain tumor enhancement in MR imaging at 3 Tesla: comparison of SNR and CNR gain using TSE and GRE techniques. *Invest Radiol*. 2007; 42(8):558–563.
2. Akeson P, Vikhoff B, Stahlberg F, et al. Brain lesion contrast in MR imaging. Dependence on field strength and concentration of gadodiamide injection in patients and phantoms. *Acta Radiol*. 1997;38(1):14–18.
3. Akeson P, Nordstrom CH, Holtas S. Time-dependency in brain lesion enhancement with gadodiamide injection. *Acta Radiol*. 1997;38(1): 19–24.
4. Vos MJ, Uitdehaag BM, Barkhof F, et al. Interobserver variability in the radiological assessment of response to chemotherapy in glioma. *Neurology*. 2003;60(5):826–830.
5. Shah GD, Kesari S, Xu R, et al. Comparison of linear and volumetric criteria in assessing tumor response in adult high-grade gliomas. *Neuro Oncol*. 2006;8(1):38–46.
6. Dempsey MF, Condon BR, Hadley DM. Measurement of tumor "size" in recurrent malignant glioma: 1D, 2D, or 3D? *AJNR Am J Neuroradiol*. 2005;26(4):770–776.
7. Provenzale JM, Ison C, Delong D. Bidimensional measurements in brain tumors: assessment of interobserver variability. *AJR Am J Roentgenol*. 2009;193(6):W515–W522.
8. Warren KE, Patronas N, Aikin AA, et al. Comparison of one-, two-, and three-dimensional measurements of childhood brain tumors. *J Natl Cancer Inst*. 2001;93(18):1401–1405.
9. Galanis E, Buckner JC, Maurer MJ, et al. Validation of neuroradiologic response assessment in gliomas: measurement by RECIST, two-dimensional, computer-assisted tumor area, and computer-assisted tumor volume methods. *Neuro Oncol*. 2006;8(2):156–165.
10. Gallego Perez-Larraya J, Lahutte M, Petrirena G, et al. Response assessment in recurrent glioblastoma treated with irinotecan-bevacizumab: comparative analysis of the Macdonald, RECIST, RANO, and RECIST + F criteria. *Neuro Oncol*. 2012;14(5):667–673.
11. Lavin PT, Flowerdew G. Studies in variation associated with the measurement of solid tumors. *Cancer*. 1980;46(5):1286–1290.
12. Fornage BD. Measuring masses on cross-sectional images. *Radiology*. 1993;187(1):289.
13. Ellingson BM, Cloughesy TF, Lai A, et al. Quantitative volumetric analysis of conventional MRI response in recurrent glioblastoma treated with bevacizumab. *Neuro Oncol*. 2011;13(4):401–409.
14. Boxerman JL, Zhang Z, Safriel Y, et al. Early post-bevacizumab progression on contrast-enhanced MRI as a prognostic marker for overall survival in recurrent glioblastoma: results from the ACRIN 6677/RTOG 0625 Central Reader Study. *Neuro Oncol*. 2013;15(7): 945–954.
15. Ellingson BM, Kim HJ, Woodworth DC, et al. Contrast-enhanced T1-weighted subtraction maps improve tumor delineation and predict survival in a multicenter clinical trial of recurrent glioblastoma treated with bevacizumab. *Radiology*. 2014;271(1): 200–210.
16. Huang RY, Rahman R, Hamdan A, et al. Recurrent glioblastoma: Volumetric assessment and stratification of patient survival with early posttreatment magnetic resonance imaging in patients treated with bevacizumab. *Cancer*. 2013;119(19):3479–3488.
17. Filippi M, Marciano N, Capra R, et al. The effect of imprecise repositioning on lesion volume measurements in patients with multiple sclerosis. *Neurology*. 1997;49(1):274–276.
18. Rohde S, Massberg M, Reinhardt J, et al. [Impact of technical and morphological factors on the precision of software-based MR tumor volumetry: a phantom study]. *Rofo*. 2008;180(7):654–661.
19. des Plantes Z. *Subtraktion*. Stuttgart: Thieme Verlag, 1961.
20. Kransdorf MJ, Murphey MD, Lee JHE, D.A. R, Imaging AMCoB. ACR-SSR Practice Guideline for the Performance and Interpretation of Magnetic Resonance Imaging (MRI) of Bone and Soft Tissue TumorsRevised 2010 - Resolution #18.
21. Suto Y, Caner BE, Tamagawa Y, et al. Subtracted synthetic images in Gd-DTPA enhanced MR. *J Comput Assist Tomogr*. 1989;13(5): 925–928.
22. Lloyd GA, Barker PG, Phelps PD. Subtraction gadolinium enhanced magnetic resonance for head and neck imaging. *Br J Radiol*. 1993;66(781):12–16.
23. Lee VS, Flyer MA, Weinreb JC, et al. Image subtraction in gadolinium-enhanced MR imaging. *AJNR Am J Roentgenol*. 1996; 167(6):1427–1432.
24. Gaul HP, Wallace CJ, Crawley AP. Reverse enhancement of hemorrhagic brain lesions on postcontrast MR: detection with digital image subtraction. *AJNR Am J Neuroradiol*. 1996;17(9): 1675–1680.

25. Melhem ER, Mehta NR. Dynamic T1-weighted spin-echo MR imaging: the role of digital subtraction in the demonstration of enhancing brain lesions. *J Magn Reson Imaging*. 1999;9(4):503–508.
26. Kaus MR, Warfield SK, Nabavi A, et al. Automated segmentation of MR images of brain tumors. *Radiology*. 2001;218(2):586–591.
27. Salman YM. Modified technique for volumetric brain tumor measurements. *J Biomed Sci Eng*. 2009;2:16–19.
28. Mazzara GP, Velthuizen RP, Pearlman JL, et al. Brain tumor target volume determination for radiation treatment planning through automated MRI segmentation. *Int J Radiat Oncol Biol Phys*. 2004;59(1):300–312.
29. Weltens C, Menten J, Feron M, et al. Interobserver variations in gross tumor volume delineation of brain tumors on computed tomography and impact of magnetic resonance imaging. *Radiother Oncol*. 2001;60(1):49–59.
30. Yamamoto M, Nagata Y, Okajima K, et al. Differences in target outline delineation from CT scans of brain tumours using different methods and different observers. *Radiother Oncol*. 1999;50(2):151–156.
31. Khoo VS, Adams EJ, Saran F, et al. A Comparison of clinical target volumes determined by CT and MRI for the radiotherapy planning of base of skull meningiomas. *Int J Radiat Oncol Biol Phys*. 2000;46(5):1309–1317.
32. Ellingson BM, Malkin MG, Rand SD, et al. Validation of functional diffusion maps (fDMs) as a biomarker for human glioma cellularity. *J Magn Reson Imaging*. 2010;31(3):538–548.
33. Sugahara T, Korogi Y, Kochi M, et al. Usefulness of diffusion-weighted MRI with echo-planar technique in the evaluation of cellularity in gliomas. *J Magn Reson Imaging*. 1999;9(1):53–60.
34. Chenevert TL, Stegman LD, Taylor JM, et al. Diffusion magnetic resonance imaging: an early surrogate marker of therapeutic efficacy in brain tumors. *J Natl Cancer Inst*. 2000;92(24):2029–2036.
35. Kidwell CS, Alger JR, Di Salle F, et al. Diffusion MRI in patients with transient ischemic attacks. *Stroke*. 1999;30(6):1174–1180.
36. Verheul HB, Balazs R, Berkelbach van der Sprenkel JW, et al. Comparison of diffusion-weighted MRI with changes in cell volume in a rat model of brain injury. *NMR Biomed*. 1994;7(1–2):96–100.
37. Farrell CJ, Hoh BL, Pisculli ML, et al. Limitations of diffusion-weighted imaging in the diagnosis of postoperative infections. *Neurosurgery*. 2008;62(3):577–583; discussion 577–583.
38. Lam WW, Poon WS, Metreweli C. Diffusion MR imaging in glioma: does it have any role in the pre-operation determination of grading of glioma? *Clin Radiol*. 2002;57(3):219–225.
39. Kono K, Inoue Y, Nakayama K, et al. The role of diffusion-weighted imaging in patients with brain tumors. *AJNR Am J Neuroradiol*. 2001;22(6):1081–1088.
40. Smith JS, Cha S, Mayo MC, et al. Serial diffusion-weighted magnetic resonance imaging in cases of glioma: distinguishing tumor recurrence from postresection injury. *J Neurosurg*. 2005;103(3):428–438.
41. Chenevert TL, McKeever PE, Ross BD. Monitoring early response of experimental brain tumors to therapy using diffusion magnetic resonance imaging. *Clin Cancer Res*. 1997;3(9):1457–1466.
42. Pope WB, Kim HJ, Huo J, et al. Recurrent glioblastoma multiforme: ADC histogram analysis predicts response to bevacizumab treatment. *Radiology*. 2009;252(1):182–189.
43. Pope WB, Qiao XJ, Kim HJ, et al. Apparent diffusion coefficient histogram analysis stratifies progression-free and overall survival in patients with recurrent GBM treated with bevacizumab: a multi-center study. *J Neurooncol*. 2012;108(3):491–498.
44. Chenevert TL, Galban CJ, Ivancevic MK, et al. Diffusion coefficient measurement using a temperature-controlled fluid for quality control in multicenter studies. *J Magn Reson Imaging*. 2011;34(4):983–987.
45. Rosen BR, Belliveau JW, Vevea JM, et al. Perfusion imaging with NMR contrast agents. *Magn Reson Med*. 1990;14(2):249–265.
46. Barajas RF Jr, Phillips JJ, Parvataneni R, et al. Regional variation in histopathologic features of tumor specimens from treatment-naive glioblastoma correlates with anatomic and physiologic MR Imaging. *Neuro Oncol*. 2012;14(7):942–954.
47. Tofts PS. Modeling tracer kinetics in dynamic Gd-DTPA MR imaging. *J Magn Reson Imaging*. 1997;7(1):91–101.
48. Detre JA, Zhang W, Roberts DA, et al. Tissue specific perfusion imaging using arterial spin labeling. *NMR Biomed*. 1994;7(1–2):75–82.
49. Mangla R, Singh G, Ziegelitz D, et al. Changes in relative cerebral blood volume 1 month after radiation-temozolomide therapy can help predict overall survival in patients with glioblastoma. *Radiology*. 2010;256(2):575–584.
50. Law M, Young RJ, Babb JS, et al. Gliomas: predicting time to progression or survival with cerebral blood volume measurements at dynamic susceptibility-weighted contrast-enhanced perfusion MR imaging. *Radiology*. 2008;247(2):490–498.
51. Cao Y, Tsien CI, Nagesh V, et al. Survival prediction in high-grade gliomas by MRI perfusion before and during early stage of RT [corrected]. *Int J Radiat Oncol Biol Phys*. 2006;64(3):876–885.
52. Barajas RF Jr, Chang JS, Segal MR, et al. Differentiation of recurrent glioblastoma multiforme from radiation necrosis after external beam radiation therapy with dynamic susceptibility-weighted contrast-enhanced perfusion MR imaging. *Radiology*. 2009;253(2):486–496.
53. Hu LS, Baxter LC, Smith KA, et al. Relative cerebral blood volume values to differentiate high-grade glioma recurrence from posttreatment radiation effect: direct correlation between image-guided tissue histopathology and localized dynamic susceptibility-weighted contrast-enhanced perfusion MR imaging measurements. *AJNR Am J Neuroradiol*. 2009;30(3):552–558.
54. Sugahara T, Korogi Y, Tomiguchi S, et al. Posttherapeutic intraaxial brain tumor: the value of perfusion-sensitive contrast-enhanced MR imaging for differentiating tumor recurrence from nonneoplastic contrast-enhancing tissue. *AJNR Am J Neuroradiol*. 2000;21(5):901–909.
55. Sawlani RN, Raizer J, Horowitz SW, et al. Glioblastoma: a method for predicting response to antiangiogenic chemotherapy by using MR perfusion imaging--pilot study. *Radiology*. 2010;255(2):622–628.
56. Sorensen AG, Batchelor TT, Zhang WT, et al. A “vascular normalization index” as potential mechanistic biomarker to predict survival after a single dose of cediranib in recurrent glioblastoma patients. *Cancer Res*. 2009;69(13):5296–5300.
57. Sorensen AG. Perfusion MR imaging: moving forward. *Radiology*. 2008;249(2):416–417.
58. Calamante F. Bolus dispersion issues related to the quantification of perfusion MRI data. *J Magn Reson Imaging*. 2005;22(6):718–722.

59. Paulson ES, Schmainda KM. Comparison of dynamic susceptibility-weighted contrast-enhanced MR methods: recommendations for measuring relative cerebral blood volume in brain tumors. *Radiology*. 2008;249(2):601–613.
60. Sugahara T, Korogi Y, Kochi M, et al. Perfusion-sensitive MR imaging of gliomas: comparison between gradient-echo and spin-echo echo-planar imaging techniques. *AJNR Am J Neuroradiol*. 2001; 22(7):1306–1315.
61. Thilmann O, Larsson EM, Bjorkman-Burtscher IM, et al. Effects of echo time variation on perfusion assessment using dynamic susceptibility contrast MR imaging at 3 tesla. *Magn Reson Imaging*. 2004;22(7):929–935.
62. Henry ME, Kaufman MJ, Lange N, et al. Test-retest reliability of DSC MRI CBV mapping in healthy volunteers. *Neuroreport*. 2001;12(8): 1567–1569.
63. Shin W, Horowitz S, Ragin A, et al. Quantitative cerebral perfusion using dynamic susceptibility contrast MRI: evaluation of reproducibility and age- and gender-dependence with fully automatic image postprocessing algorithm. *Magn Reson Med*. 2007;58(6):1232–1241.
64. Jackson A, Kassner A, Zhu XP, et al. Reproducibility of T2* blood volume and vascular tortuosity maps in cerebral gliomas. *J Magn Reson Imaging*. 2001;14(5):510–516.
65. Ellingson BM, Zaw T, Cloughesy TF, et al. Comparison between intensity normalization techniques for dynamic susceptibility contrast (DSC)-MRI estimates of cerebral blood volume (CBV) in human gliomas. *J Magn Reson Imaging*. 2012;35(6):1472–1477.
66. Alger JR, Schaewe TJ, Lai TC, et al. Contrast agent dose effects in cerebral dynamic susceptibility contrast magnetic resonance perfusion imaging. *J Magn Reson Imaging*. 2009;29(1):52–64.
67. Knutsson L, Lindgren E, Ahlgren A, et al. Dynamic susceptibility contrast MRI with a prebolus contrast agent administration design for improved absolute quantification of perfusion. *Magn Reson Med*. 2013. doi: 10.1002/mrm.25006.
68. Hu LS, Baxter LC, Pinnaduwage DS, et al. Optimized preload leakage-correction methods to improve the diagnostic accuracy of dynamic susceptibility-weighted contrast-enhanced perfusion MR imaging in posttreatment gliomas. *AJNR Am J Neuroradiol*. 2010;31(1):40–48.
69. Boxerman JL, Prah DE, Paulson ES, et al. The Role of preload and leakage correction in gadolinium-based cerebral blood volume estimation determined by comparison with MION as a criterion standard. *AJNR Am J Neuroradiol*. 2012;33(6):1081–1087.
70. Boxerman JL, Schmainda KM, Weisskoff RM. Relative cerebral blood volume maps corrected for contrast agent extravasation significantly correlate with glioma tumor grade, whereas uncorrected maps do not. *AJNR Am J Neuroradiol*. 2006;27(4): 859–867.
71. Calamante F, Gadian DG, Connelly A. Quantification of perfusion using bolus tracking magnetic resonance imaging in stroke: assumptions, limitations, and potential implications for clinical use. *Stroke*. 2002;33(4):1146–1151.
72. Wu O, Ostergaard L, Weisskoff RM, et al. Tracer arrival timing-insensitive technique for estimating flow in MR perfusion-weighted imaging using singular value decomposition with a block-circulant deconvolution matrix. *Magn Reson Med*. 2003;50(1):164–174.
73. Mouridsen K, Friston K, Hjort N, et al. Bayesian estimation of cerebral perfusion using a physiological model of microvasculature. *Neuroimage*. 2006;33(2):570–579.
74. Mukherjee P, Kang HC, Videen TO, et al. Measurement of cerebral blood flow in chronic carotid occlusive disease: comparison of dynamic susceptibility contrast perfusion MR imaging with positron emission tomography. *AJNR Am J Neuroradiol*. 2003; 24(5):862–871.
75. Bedekar D, Jensen T, Schmainda KM. Standardization of relative cerebral blood volume (rCBV) image maps for ease of both inter- and intrapatient comparisons. *Magn Reson Med*. 2010;64(3): 907–913.
76. Wetzel SG, Cha S, Johnson G, et al. Relative cerebral blood volume measurements in intracranial mass lesions: interobserver and intraobserver reproducibility study. *Radiology*. 2002;224(3): 797–803.
77. Committee DMT. DCE MRI Quantification Profile 2012.
78. OMIM. Online Mendelian Inheritance in Man Database. Available at http://www.ncbi.nlm.nih.gov/omim. Accessed February 28, 1998.
79. Ferl GZ, Xu L, Friesenhahn M, et al. An automated method for nonparametric kinetic analysis of clinical DCE-MRI data: application to glioblastoma treated with bevacizumab. *Magn Reson Med*. 2010;63(5):1366–1375.
80. Roberts C, Issa B, Stone A, et al. Comparative study into the robustness of compartmental modeling and model-free analysis in DCE-MRI studies. *J Magn Reson Imaging*. 2006; 23(4):554–563.
81. Jackson A, Jayson GC, Li KL, et al. Reproducibility of quantitative dynamic contrast-enhanced MRI in newly presenting glioma. *Br J Radiol*. 2003;76(903):153–162.
82. Di Chiro G, DeLaPaz RL, Brooks RA, et al. Glucose utilization of cerebral gliomas measured by [18F] fluorodeoxyglucose and positron emission tomography. *Neurology*. 1982;32(12): 1323–1329.
83. Isselbacher KJ. Sugar and amino acid transport by cells in culture--differences between normal and malignant cells. *N Engl J Med*. 1972;286(17):929–933.
84. Souba WW. Glutamine and cancer. *Ann Surg*. 1993;218(6): 715–728.
85. Lilja A, Bergstrom K, Hartvig P, et al. Dynamic study of supratentorial gliomas with L-methyl-11C-methionine and positron emission tomography. *AJNR Am J Neuroradiol*. 1985;6(4): 505–514.
86. Go KG, Keuter EJ, Kamman RL, et al. Contribution of magnetic resonance spectroscopic imaging and L-[1–11C]tyrosine positron emission tomography to localization of cerebral gliomas for biopsy. *Neurosurgery*. 1994;34(6):994–1002; discussion 1002.
87. Popperl G, Gotz C, Rachinger W, et al. Value of O-(2-[18F]fluoroethyl)- L-tyrosine PET for the diagnosis of recurrent glioma. *Eur J Nucl Med Mol Imaging*. 2004;31(11): 1464–1470.
88. Heiss WD, Wienhard K, Wagner R, et al. F-Dopa as an amino acid tracer to detect brain tumors. *J Nucl Med*. 1996;37(7): 1180–1182.
89. Beuthien-Baumann B, Bredow J, Burchert W, et al. 3-O-methyl-6-[18F]fluoro-L-DOPA and its evaluation in brain tumour imaging. *Eur J Nucl Med Mol Imaging*. 2003;30(7):1004–1008.
90. Becherer A, Karanikas G, Szabo M, et al. Brain tumour imaging with PET: a comparison between [18F]fluorodopa and [11C]methionine. *Eur J Nucl Med Mol Imaging*. 2003;30(11):1561–1567.
91. Pauleit D, Floeth F, Hamacher K, et al. O-(2-[18F]fluoroethyl)-L-tyrosine PET combined with MRI improves the diagnostic assessment of cerebral gliomas. *Brain*. 2005;128(Pt 3):678–687.

92. Fueger BJ, Czernin J, Cloughesy T, et al. Correlation of 6–18F-fluoro-L-dopa PET uptake with proliferation and tumor grade in newly diagnosed and recurrent gliomas. *J Nucl Med*. 2010;51(10):1532–1538.

93. Dunet V, Rossier C, Buck A, et al. Performance of 18F-fluoro-ethyl-tyrosine (18F-FET) PET for the differential diagnosis of primary brain tumor: a systematic review and Metaanalysis. *J Nucl Med*. 2012;53(2):207–214.

94. Singhal T, Narayanan TK, Jacobs MP, et al. 11C-methionine PET for grading and prognostication in gliomas: a comparison study with 18F-FDG PET and contrast enhancement on MRI. *J Nucl Med*. 2012;53(11):1709–1715.

95. Cameron IL, Smith NK, Pool TB, et al. Intracellular concentration of sodium and other elements as related to mitogenesis and oncogenesis in vivo. *Cancer Res*. 1980;40(5):1493–1500.

96. Ouwerkerk R, Bleich KB, Gillen JS, et al. Tissue sodium concentration in human brain tumors as measured with 23Na MR imaging. *Radiology*. 2003;227(2):529–537.

97. Nagel AM, Bock M, Hartmann C, et al. The potential of relaxation-weighted sodium magnetic resonance imaging as demonstrated on brain tumors. *Invest Radiol*. 2011;46(9):539–547.

98. Wen Z, Hu S, Huang F, et al. MR imaging of high-grade brain tumors using endogenous protein and peptide-based contrast. *Neuroimage*. 2010;51(2):616–622.

99. Jin T, Wang P, Zong X, et al. Magnetic resonance imaging of the Amine-Proton EXchange (APEX) dependent contrast. *Neuroimage*. 2012;59(2):1218–1227.

100. Sun PZ, Benner T, Copen WA, et al. Early experience of translating pH-weighted MRI to image human subjects at 3 Tesla. *Stroke*. 2010;41(10 Suppl):S147–S151.